The Effects of Aging on the Material Properties of Human Costal Cartilage

A. G. Lau[1], J. M. Mattice[1], D. Murakami[2], M. L. Oyen[1], and R. W. Kent[1]
[1] University of Virginia; [2]Nissan Motor Corporation

ABSTRACT

Understanding the mechanical properties of the aging thorax is important in the development of restraint systems to protect the older population. This study investigated how the material properties of costal cartilage change with age. Indentation testing was used to study the material properties of human costal cartilage. Ribcages were obtained from 11 human subjects ranging in age from 23 to 77 years. Costal cartilage from the second, third, and fourth left ribs were excised and prepared into 6 mm thick cross sections. The cross sections were tested using spherical indentation with a ramp-hold relaxation test. Shear and elastic moduli were calculated from the stress relaxation response. The results showed only a slight trend of increasing costal cartilage stiffness with age and there was a larger overall standard deviation in the older specimen values. Differences were observed during specimen preparation which included changes in color, increasing inhomogeneity, and varying regions of calcification. Calcification was observed as shells surrounding the softer cartilage, as well as calcified strata running transversely through the interior of the cartilage. These regions should affect the overall mechanical response during thoracic loading, but were not as apparent in the results of the current study because the indentation area was localized near the center of the cartilage cross sections.

INTRODUCTION

Older drivers (65+) are more prone to chest injuries in automotive crashes (Morris *et al.*, 2002). It has also been found that older drivers are more likely to die from chest injuries than younger drivers. (Kent *et al*., 2005a). Recent efforts have focused on the characterization of the rib bone on a structural level (Charpail, *et al.,* 2005) and on the material level (Stitzel *et al*., 2003, Kemper *et al.,* 2005). Further research has been done to track how the rib cage geometry changes with age (Kent *et al*., 2005b). By gaining a better understanding of the aging thorax, new measures can be taken to help protect these older occupants.

One factor that could have an impact on the overall behavior of the thorax is the mechanical properties of the costal cartilage, which connect the rib bones to the sternum. The costal cartilage is similar to the articular cartilage in that they are both from the hyaline cartilage family. The costal cartilage has been known to calcify with increasing age (Teale *et al*., 1989). Also, the "amianthoid change" occurs in aging costal cartilage, where the collagen fibrils become more oriented (Hukins *et al*., 1976). Changes in the costal cartilage caused by calcification and amianthoid change could have effects on the overall mechanical behavior of the ribcage. Because of the clinical drive from osteoarthritis, there has been extensive mechanical characterization of the articular cartilage. On the other hand, little work has been done performed on costal cartilage, and how the mechanical properties of the costal cartilage change with age is unknown.

Indentation testing is a common method for material characterization (Johnson, 1985). A probe with a defined geometry (flat, spherical, pyramidal, conical) is brought into contact with the sample and is performed with displacement or force control. This type of testing has advantages over traditional tensile testing, especially for biological materials, where it is difficult to prepare specimens into tensile bars. This study examined how the mechanical behavior of human costal cartilage changes with age through spherical indentation testing.

METHODS

Equipment Specifications

Indentation tests were performed using a custom-built, displacement-controlled indentation system. A high precision table Industrial Devices Corporation (IDC) Model RB6 driven by an IDC Model B23 Brushless Servo Motor was mounted to a Palmgren Rotary Table Model 84. This allowed for precise displacement control along the z-axis. An indentation assembly was built and mounted to the linear actuator of the IDC table. This assembly contained mounting locations for a position transducer (Nototechnik Model T25) and a load cell. A 10-pound load cell (Sensotec Model 31) and hemi-spherical indenter tip (3.15 mm diameter) were mounted in-line at the end of this assembly.

All data was recorded using a National Instruments (NI) data acquisition setup. This setup consisted of a computer with an internal NI DAQ PCI card (Model PCI-MIO-16E-4). This

DAQ card connected externally to a custom breakout box which housed the interface for the data channel inputs. A custom program written in LabVIEW 7 was used for data acquisition.

Cadaveric(subject) Specimens

Rib cages from eleven cadaveric subjects were obtained for this study. These subjects included both males and females and ranged in age from 23 to 77 years. The specimen information is outlined below in Table 1.

Table 1: Cadaver Specimen Details

Sex	Age	Height (cm)	Weight (kg)	BMI	Body type	Cause of Death
M	23	182.9	91.6	27.4	Overweight	Schizophrenia, leukemia
F	32	169	83.9	29.4	Overweight	Cancer
F	38	163	94.8	35.7	Severely Obsese	Sepsis
F	42	176.5	54.4	17.5	Underweight	N/A
M	47	170.5	47.6	16.4	Underweight	Complications of chronic alcoholism
F	49	173	95	31.7	Overweight	N/A
M	53	179.8	87.1	26.9	Overweight	Respiratory failure
F	61	173.2	80.7	26.9	Overweight	Pulmonary edema
F	67	166.3	79.8	28.9	Overweight	Lung cancer
F	75	170.5	46.7	16.1	Underweight	Polycythemia vera
M	77	184	122	36.0	Severely Obsese	Cardiopulmonary arrest

Specimen Preparation

Each rib cage were removed from the freezer and allowed to thaw. Any excess tissue and fat were removed in order to better locate the 2^{nd}, 3^{rd}, and 4^{th} left ribs. To remove these ribs, an autopsy bone saw was used to make a cut mid sternum from the 2^{nd} to 4^{th} rib and through the ribs lateral to the osteochondral joint. The remaining tissue was removed from the ribs and then the sternum was separated from the rib at the costosternal joint.

Using a custom cutter having parallel utility knife blades, the costal cartilage from each rib was sectioned into 6-mm thick cross sections starting from the sternum moving toward the osteochondral joint at the rib. Section 1 began after the costosternal joint, which was not used for testing. To ensure a uniform thickness from the cutter's parallel blades, there was a thin separation between each section. Between three and seven sections of the costal cartilage were prepared from each rib depending on sample size. In order to keep track of the medial face of each section, that edge was marked with India ink.

Slice thickness (t), distances along the major and minor axes, and distance between sections (d) were measured with digital calipers. The medial and lateral faces of each section were photographed and then the cartilage sections were soaked in 0.9% physiological saline for at least 30 minutes prior to testing.

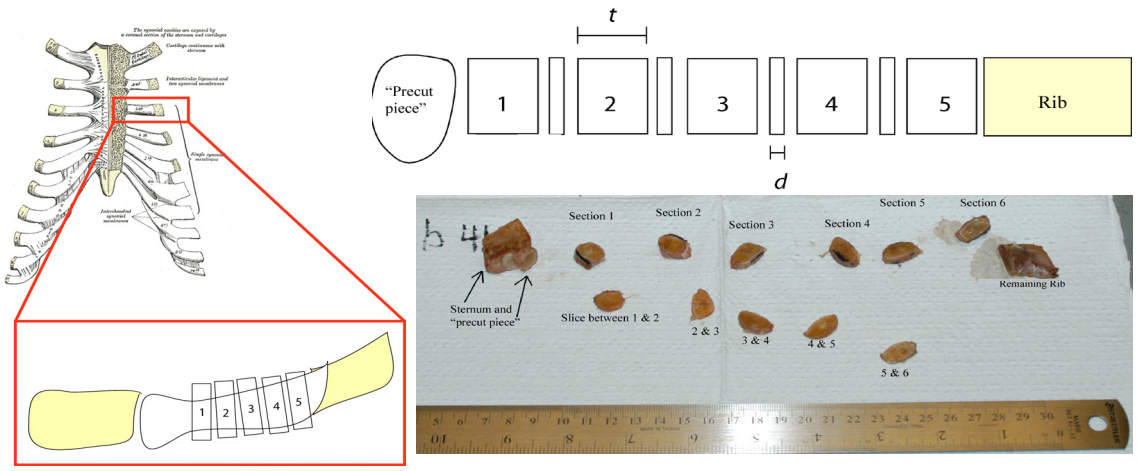

Figure 1: A diagram of how the costal cartilage cross sections were prepared.

Specimen Testing

During indentation testing, the samples were held in a custom holder and bathed in 0.9% physiological saline at room temperature. Indentation tests were performed at the center on the medial face of each cartilage cross-section. A ramp-hold displacement profile with a target rise time of t_R = 2.125 s and target peak displacement of h_{max} = 0.425 mm. By keeping the indentation depth to less than 10% of the sample thickness, the cartilage sections can be treated as a bulk medium (Oliver and Pharr, 1992). The contact point was determined by adjusting the displacement position by hand to a preload force of 0.05 Newtons. After the contact point was determined, an automated IDC program was run to produce the displacement profile shown in Figure 2 (Right). This profile consisted of an upward displacement of 0.5 mm with a 5 second hold followed by a 0.925 mm downward displacement followed by a 120 second hold. This gives a net downward displacement of 0.425 mm from the contact point. Using this profile eliminates the inertial effects of starting the downward displacement from the contact point.

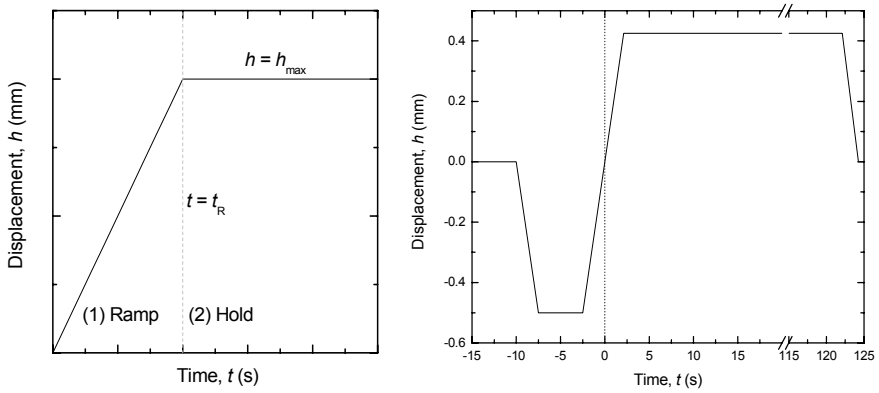

Figure 2: (Left) Ramp-hold displacement profile used for analysis. (Right) Programmed experimental machine displacement profile

Because of the inhomogeneity of the cartilage cross sections, sometimes there would be other locations of interest for indentation which were not located near the center. In this case, a second indentation test on the specimen would be performed, but only after all the specimens for the day had been tested once. This ensured that the cartilage specimen had adequate time (at least 20 minutes) to return to its original state (Wang, *et al.,* 2003).

Data Post-Processing

A custom Visual Basic script in Microsoft Excel was used to process the raw data output from LabVIEW. This included debiasing the force and displacement channels and data decimation by a level crossing algorithm. The decimation algorithm recorded data points in the force channel whenever the value changed more than 0.04 Newtons from the previous recorded value. The macro also identified the contact point with a 4-point rolling average of force exceeded 0.03 Newtons. The experimental rise time (t_R) and indentation depth (h_{max}) were calculated from the time and displacement values at this contact point.

Data Analysis

Based on the Hertzian solution for a sphere (Johnson, 1985), the parameters from a relaxation function can be found using spherical indentation under step loading (Cheng *et al.*, 2005). However, an instantaneous step is not possible in experimentation, and in reality, is a ramp-hold displacement profile (Figure 2). Because no solution exists for displacement controlled spherical indentation with a ramp hold input (Sakai*,* 2002), the Mattice *et al.* (2006) analysis method, which takes into account this non-zero rise time (t_R) was used to find the relaxation function parameters of the relaxation function $G(t)$. A three-time constant model for a viscoelastic solid was used.

$$G(t) = C_0 + C_1 \exp(-t/\tau_1) + C_2 \exp(-t/\tau_2) + C_3 \exp(-t/\tau_3) \qquad \text{(Eqn. 1)}$$

And the instantaneous (G_0) and long time (G_∞) shear modulus values were calculated from the parameters in (Eqn. 1). Assuming incompressibility ($\nu = 0.5$), the elastic modulus values can be calculated from the shear modulus values using $E = 3G$.

RESULTS

The mean (± standard deviation) thickness of all the sections prepared was 5.967 (± 0.557) mm. For all the indentation tests, the mean rise time was 2.225 (± 0.126) seconds and mean displacement was 0.448 (± 0.028) mm.

The shear modulus values obtained from the 188 indentation tests are shown in Figure 3. As an entire group, there were no statistically significant trends with age. Analysis of just the male subjects showed an increasing trend with age for G_0, G_∞, and G_∞/G_0. While, analysis of just the female subjects showed a decreasing trend in G_∞/G_0.

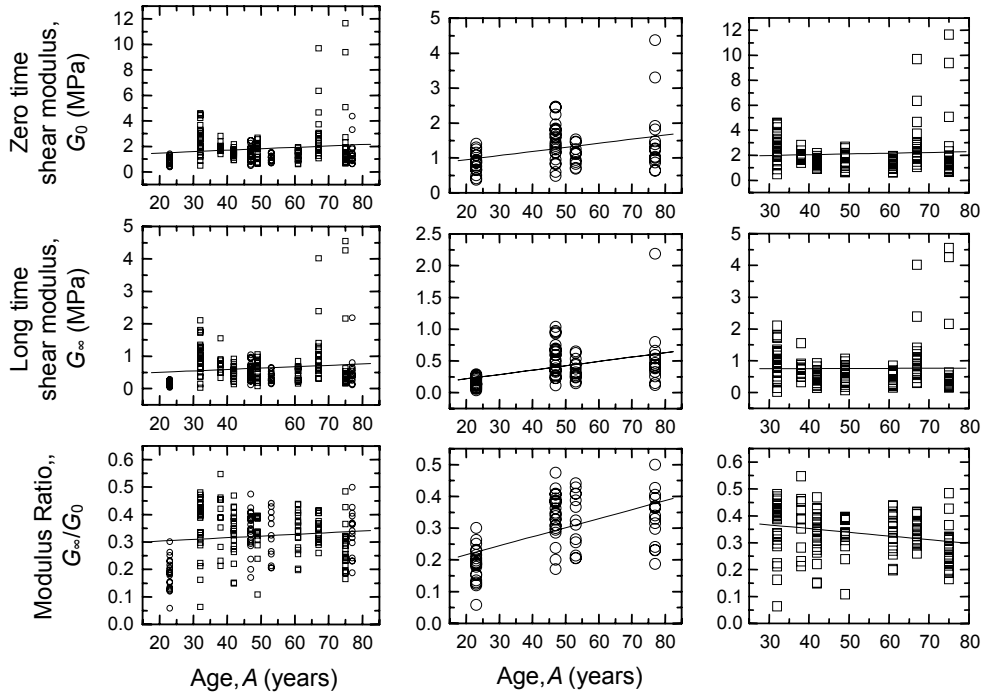

Figure 3: Modulus (G_0, G_∞) and modulus ratio (G_∞ / G_0) plotted as a function of age. Male subjects are denoted by a ○ and female subjects are denoted by a □. Solid lines are the linear regression fits, with the R and p-values included in Table 2. (Left) All Subjects. (Center) Male only. (Right) Female only

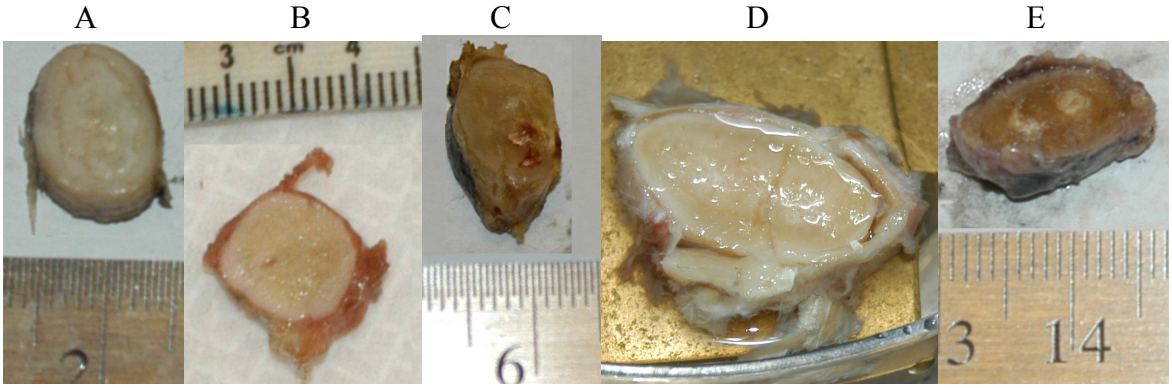

*Ruler Scale in cm. Small marks are 0.5 or 1.0 mm

Figure 4: From Left to Right. Costal Cartilage Sections From:
A. 23 – Male. Note the homogenous white color of the cartilage
B. 32 – Female. Note the center is beginning to turn a yellowish color
C. 47 – Male. Calcification Spots and evidence of vascularization seen inside the cartilage
D. 53 – Male. There is a calcification shell around the cartilage, which is starting to separate.
E. 75 – Female. Shows two areas of calcification (white spots on interior)

Table 2: Linear Regression results from data plotted in Figure 3.

	R	p-value	+ or – correlation
G_0 –All	0.14	0.05	+
G_0 –M	0.34	<0.01*	+
G_0 –F	0.06	0.49	+
G_∞ –All	0.12	0.09	+
G_∞ –M	0.41	<0.01*	+
G_∞ –F	<0.01	0.92	+
G_∞ / G_0 –All	0.11	0.11	+
G_∞ / G_0 –M	0.54	<0.01*	+
G_∞ / G_0 –F	0.25	<0.01*	–

*Statistical significance

SUMMARY AND DISCUSSION

Overall, the instantaneous elastic modulus (E_0) ranged from 1.1 to 34.1 MPa and the long-time (relaxed) elastic modulus (E_∞) ranged from 0.1 to 13.3 MPa. At the low end, these values are within the range of the known values for articular cartilage in compression around 0.3 to 1.5 MPa (Laasanen *et al.*, 2003). Although there was only a slight trend (p = 0.05) of stiffening costal cartilage with increasing age, many changes in the costal cartilage were observed visually during the specimen preparation process (Figure 4). These included changes in midsubstance color, various regions of calcification, areas of vascularization, and increasing inhomogeneity within the costal cartilage.

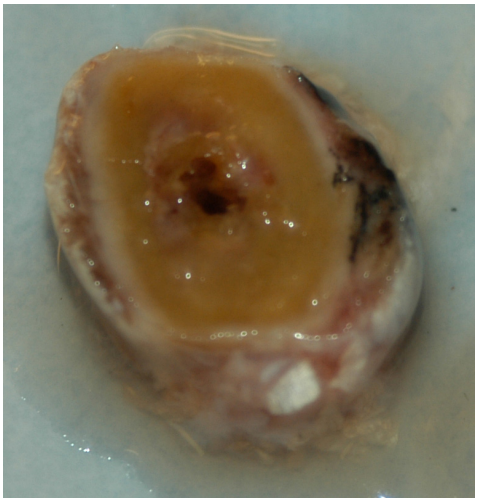

Figure 5: Section 1 of the 2nd Left Rib from the 75-female specimen. There is shell calcification along the left and lower right outer edges and a vascularized calcification hole in the middle.

There were two varieties of calcification observed during the study. One was a shell type calcification which would run along the outer edge of the costal cartilage. The degree of calcification shell ranged from being a thin layer (Figure 5), to completely surrounding the costal cartilage (Figure 4-D). The other type is calcified "strata" that ran transversely through the interior of the cartilage and may or may not have vascularization (Figure 4- C&E).

One of the most interesting aspects of Figure 4-E, which shows the medial face of section 6 from rib 4, is that the calcification strata were traced from the lateral face of section 6 all the way to the medial face of section 4. This allowed the opportunity to test these calcified regions in isolation without the layering effect of the underlying cartilage. These targeted tests of sections 5 and 6 produced the first and third largest stiffness values from the entire study (Peak load of 14.95 and 12.28 Newtons, E_0 = 34.1 and 27.5 MPa, and E_∞ = 12.5 and 13.3 MPa respectively). In addition, the test on section 4, whose force-time plot is shown in Figure 6, would have yielded even higher values but could not be analyzed due to the fracture during the test. The second highest value came from section 5 of rib 4 from the 67-female specimen, which also contained this type of interior calcification strata. The modulus values from these tests fall within the range of the calcified zone of (knee) articular cartilage which was found to range from 10-100 times stiffer than the normal cartilage (Mente, *et al.* 1994). Although it has also been found that the calcified cartilage can be on the same order of magnitude as the subchondral bone (Ferguson *et al.,* 2003).

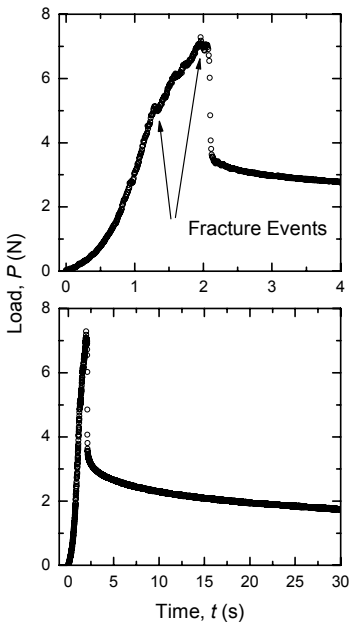

Figure 6: A raw load-time (*P*-*t*) response for an indentation test in which there were apparent fracture events, both on loading and at the onset of relaxation (75-female, Rib 4 Section 4). (Top) Zoomed on the loading portion of the curve shown on bottom.

While there were some instances of calcification running through the interior midsubstance of the costal cartilage, the majority of the calcification was observed as an outer shell. Due to the central placement of our tests, these calcification regions had little influence on our experiment results. For example, even though the largest modulus values came from the 75-female specimen, the 77-male specimen had an outer calcification shell that was so hard, that the knife blade was unable to even penetrate it, and an autopsy bone saw had to be used. Although not apparent from the results of the current study, these regions would have significant effects on

the overall rib cage behavior as they would be areas for stress concentration during thoracic loading in automotive accidents. An alternative method that would allow indentations near the edge would be using a smaller indenter tip with cartilage cross sections that were embedded in resin. Also, the costal cartilage could be embedded and indented on the exterior surface.

One limitation of the study includes the possible effects from freezing and thawing the cartilage prior to specimen preparation and testing. Also, indentation tests provide information for the compressive behavior and studies of articular cartilage have shown differences in compressive and tensile behavior (Wilson *et al,* 2005). In addition, the results could be skewed by any outliers because there were only 11 specimens in the study.

Future work could implement micro CT (Computed Tomography) analysis, which has been used to study osteoarthritis and is considered the gold standard for imaging bone microstructure (Chappard *et al*., 2005). Detailed 3-Dimensional images with down to 10μm isotropic voxel resolution can be created. CT has been used to study the calcification of aortic valves (Boxt, 2004) and would be a very useful tool for studying the progression of calcification in costal cartilage. This would allow for comparison between the calcifying cartilage and the neighboring rib bone. In addition, pre-scans would allow for special specimen preparation to target specific regions of calcification for mechanical testing.

In conclusions, the results from this study did not show a significant trend of stiffening costal cartilage with age. While the costal cartilage itself may not have significant effects, the observed calcification shells and strata would definitely have an impact on the ribcage behavior. Studying how the effects from this calcification and how it progresses will aid in the development of safer restraint systems for the elderly to help prevent potential deadly chest injuries.

ACKNOWLEDGEMENTS

The authors would like to thank the staff of the University of Virginia Center for Applied Biomechanics, especially Matt Kindig for his assistance in specimen preparation. The funds for this project were provided by Nissan Motor Corporation. The opinions expressed in this paper are the opinions of the authors alone and do not necessarily represent the views of the sponsoring organization.

REFERENCES

BOXT, L.M., (2005). CT of Valvular Heart Disease. International Journal of Cardiovascular Imaging. 21:105-113.

CHAPPARD, C., PEYRIN, F., BONNASSIE, A., LEMINEUR, G., BRUNET-IMBAULT, B., LESPESSAILLES, E., BENHAMOU, C.-L., (2006). Subchondral bone micro-architectural alterations in osteoarthritis: a synchrotron micro-computer tomography study, Osteoarthritis and Cartilage. 14:215-223

CHARPAIL, E., TROSSEILLE, X., PETIT, P., LAPORTE, S., LAVASTE, F., VALLANCIEN, G., (2005). Characterization of PMHS Ribs: A New Test Methodology. Stapp Car Crash Journal. 49:183-198.

CHENG, L., XIA, X., SCRIVEN, L.E., GERBERICH, W.W., (2005) Spherical-tip Indentation of Viscoelastic Material. Mechanics of Materials. 37:213-226

FERGUSON, V.L., BUSHBY, A.J., BOYDE, A., (2003). Nanomechanical Properties and Mineral Concentration in Articular Calcified Cartilage and Subchondral Bone. J. Anat. 203:191-202

HUKINS, D.W., KNIGHT, D.P., WOODHEAD-GALLOWAY, J. (1976) Amianthoid Change: Orientation of Normal Collagen Fibrils During Aging. Science, Nov 5; Vol.194(4265): 622-624

JOHNSON, K.L., (1985) Contact Mechanics. UK: Cambridge University Press, © 1985

KEMPER, A.R., MCNALLY, C., KENNEDY, E.A., MANOOGIAN, S.J., RATH, A.L., NG, T.P., STITZEL, J.D., SMITH, E.P., DUMAS, S.M., MATSUOKA, F. (2005). Material Properties of Human Rib Cortical Bone from Dynamic Tensions Coupon Testing. Stapp Car Crash Journal. 49:199-230.

KENT, R.W., HENARY, B., (2005a). On the Fatal Crash Experience of Older Drivers. Proc. Association for the Advancement of Automotive Medicine (AAAM). 49:371-391.

KENT, R.W., LEE, S., DARVISH, K., WANG, S., POSTER, C., LANGE, A., BREDE, C., LANGE, D., MATSUOKA, F. (2005b) Structural and Material Changes in the Aging Thorax and Their Role in Reduced Thoracic Injury Tolerance. Stapp Car Crash Journal 49:231-249.

LAASANEN, M.S, TOYRAS, J., KORHONEN, R.K., RIEPPO, J., *et al.* (2003) Biomechanical Properties of Knee Articular Cartilage. Biorheology. 40:133-140

LEE, E.H., RADOK J.R.M., (1960). Contact Problem for Viscoelastic bodies. Journal of Applied Mechanics 1960, 27:438-44

MATTICE, J.M., LAU, A.G., OYEN, M.L, KENT, R.W., (2006) Spherical Indentation Load-Relaxation of Soft Biological Tissues. Journal of Materials Research. In Press.

MENTE, P.L., LEWIS, J.L., (1994). Elastic Modulus of Calcified Cartilage is an Order of Magnitude Less than that of Subcondral Bone. J. Orthop. Res., Sept;12(5):637-47.

MORRIS, A., WELSH, R., FRAMPTON, R., CHARLTON, J., FILDES, B., (2002). An Overview of Requirements for the Crash Protection of Older Drivers. Proc. AAAM, 46:141-156.

OLIVER, W.C., PHARR, G.M., (1992). Improved Technique for Determining Hardness and Elastic Modulus Using Load and Displacement Sensing Indentation Experiments, Journal of Materials Research 1992, 7(6):1564-83.

SAKAI, M., (2002). Time-dependent Viscoelastic Relation Between Load and Penetration for an Axisymmetric Indenter. Philosophical Magazine. Vol. 82, No 10: 1841-1849.

STITZEL, J.D., CORMIER, J.M., BARRETTA, J.T., KENNEDY, E.A., SMITH E.P., RATH, A.L., DUMA, S.M., MATSUOKA, F. (2003) Defining Regional Variation in the Material Properties of Human Rib Cortical Bone and its Effect on Fracture Prediction. Stapp Car Crash Journal 2003; 47:243-65.

TEAL, C., ROMANIUK, C., MULLEY, G., (1989). Calcification on Chest Radiographs: The Association with Age. Age and Aging, 18:333-336

WANG, C.C-B., CHAHINE, N.O., HUNG, C.T., ATESHIAN, G.A., (2003). Optical Determination of Anisotropic Material Properties of Bovine Articular Cartilage in Compression. Journal of Biomechanics, 2003, 36:339-353.

WILSON, W., VAN DONKELAAR, C.C., VAN RIETBERGEN, R., HUISKES, R., (2005). The Role of Computational Models in the Search for the Mechanical Behavior and Damage Mechanisms of Articular Cartilage. Medical Engr. & Physics. 27:810-826.

AUTHOR LIST

1. Anthony G. Lau
   1011 Linden Ave, Charlottesville, VA 22902
   Phone: 434-296-7288 ext 117
   E-mail: ALau@virginia.edu

2. Jason Mattice
   1011 Linden Ave, Charlottesville, VA 22902
   Phone: 434-296-7288
   E-mail: jmm8vy@virginia.edu

3. Daisuke Murakami
   Technology Research Laboratory No.4, NISSAN MOTOR CO., LTD. 1 Natsushima-cho, Yokosuka, 237-8523
   Phone: +81-46-867-5157
   E-mail: d-murakami@mail.nissan.co.jp

4. Michelle Oyen
   1011 Linden Ave, Charlottesville, VA 22902
   Phone: 434-296-7288 ext 164
   E-mail: mloyen@virginia.edu

5. Rich Kent
   1011 Linden Ave, Charlottesville, VA 22902
   Phone: 434-296-7288 ext 133
   E-mail: rwk3c@virginia.edu